

Review

Review of the current transducer techniques

Chunjun Tang¹ · Jiakai Liang¹ · Qiang Zhu¹ · Xiaofeng Lu² · Jun Shu² · Cong Jiang³

Received: 20 April 2024 / Accepted: 24 June 2024

Published online: 26 June 2024

© The Author(s) 2024 [OPEN](#)

Abstract

Current measurement technologies encompass a wide array of techniques, numbering over ten distinct methods. Among these, current sensors such as Rogowski coils and transformers based on Ampere's law stand out. These sensors utilize electrical insulation between the primary and secondary windings, ensuring accurate and safe current measurement. In practical applications, current sensors play a critical role across various industries. They have become indispensable components in numerous devices, including inverters, DC/DC converters, motor controllers, uninterruptible power supplies, switch-mode power supplies, process control systems, and battery management systems. However, the high performance of these sensors often comes with increased costs, necessitating a thorough exploration of their notable advantages and inherent limitations. This paper aims to provide a detailed overview of the working principles and applications of various current sensors. By offering a clearer understanding of the different operating modes of these sensors and their respective strengths and limitations in practical applications, this paper seeks to furnish subsequent researchers with valuable insights for future investigations.

Keywords Ampere law · Current measurement · Current sensors · Working principles

Abbreviations

| | |
|--------|--|
| A/D | Analog-to-digital converter |
| DSP | Digital signal processing |
| MEMS | Micro-electro-mechanical system |
| PCB | Printed circuit board |
| SMDCSR | Surface-Mounted Distributed Coaxial Structure Resistor |
| MR | Magneto resistive |
| AMR | Anisotropic magneto resistance |
| GMR | Giant magneto resistive |
| TMR | Tunnel magneto resistance |
| NMR | Nuclear magnetic resonance |
| HECS | Hall effect current sensor |
| HCT | Hall effect current transformer |
| CT | Current transformer |
| HDD | Hard disk drive |

✉ Cong Jiang, jc1998hub@gmail.com; Chunjun Tang, 165513505@qq.com; Jiakai Liang, 1jk894402774@qq.com; Qiang Zhu, 59087968@qq.com; Xiaofeng Lu, 82846056@qq.com; Jun Shu, juner_83@sina.com | ¹State Grid Zhejiang Electric Power Company Jinhua Power Supply Company, Jinhua 321000, People's Republic of China. ²Sanwei Electric Power Branch of Jinhua Power Transmission and Transformation Engineering Co., Ltd, Jinhua 32100, People's Republic of China. ³School of Microelectronics, Hubei University, Wuhan 430062, Hubei, People's Republic of China.



MTJ Magnetic tunnel junction
B Magnetic induction strength

1 Introduction to current measurement technology

Current measurement technology encompasses a wide array of techniques, each varying in complexity, performance, and cost. Current sensors, such as Rogowski coils and transformers based on Ampere's law, feature electrical insulation between primary secondary windings. These sensors meet industrial requirements and find extensive applications in inverters, DC/DC converters, motor controllers, uninterrupted power supplies, switch-mode power supplies, process control, and battery management systems.

The accurate measurement of current, as a fundamental physical quantity, holds significant importance. Over time, for measuring current have evolved, from flow diverters employed in the 1880s to modern methods based on magnetoresistive effects and MEMS technology. This evolution has led to improved and decreased costs in current measurement products.

Current sensors play a crucial role in real-time monitoring protection of machinery and systems by indirectly measuring current through detection of the magnetic field generated by the original current. They provide voltage or current output, which can be directly applied to a system or converted into a digital signal for processing by microprocessors or DSPs.

These sensors are utilized in various industries, including traditional sectors and emerging fields like renewable energy and automation systems. Different applications require different sensor specifications, such as accuracy, response time, and interference resistance, current sensors based on various technologies have been developed to meet diverse requirements.

In summary current sensors based on different physical principles offer a range of capabilities, including different measurement ranges, accuracies, bandwidths insulation, response speeds, interference resistance, and costs. The advancement of current measurement technology continues drive improvements in performance and ability across various industrial domains. This paper explores current dividers based on Ohm's Law and current sensors based on Ampère's Law.

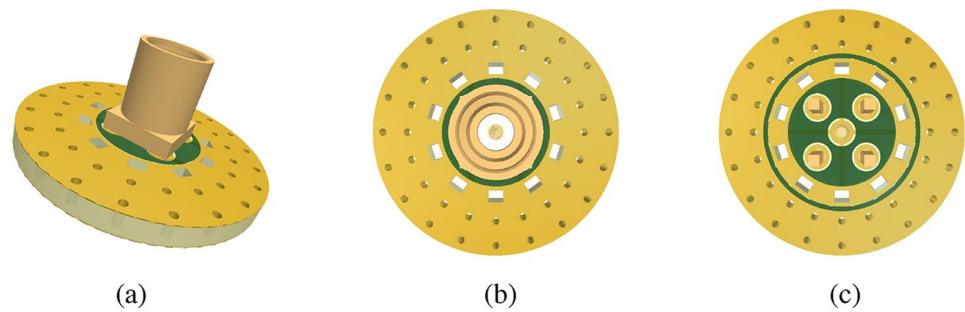
The first type of current sensor is a shunt, which is based on Ohm's law. The output voltage and measured current at both ends of the shunt are proportional. This type of sensor has the advantages of being low-cost and easy to use, and it can meet general requirements for current measurement applications. However, the shunts are in series in the circuit, which leads to significant limitations, such as large losses and no electrical insulation when measuring large currents. Therefore, when used in an environment that requires electrical insulation, additional measures must be taken, such as isolated amplifiers, which result in higher costs and lower bandwidth. High-performance current sensors are being developed, such as coaxial current sensors and so on [1].

Currently, the cutting-edge coaxial shunt resistors employ a coaxial structure, effectively eradicating magnetic flux coupling between the power and measurement loops, boasting a measurement bandwidth of up to 2.0 GHz [2]. However, the presence of a parasitic inductance of approximately 2.2 nH poses a potential detriment to the precision and efficacy of measurements [3]. In order to mitigate the impact of larger parasitic inductance, endeavors have been made to utilize compact surface mount resistors, particularly thin-film resistors where the resistor material is thinly deposited onto a ceramic substrate [4]. The incorporation of a ceramic substrate serves to adeptly absorb and disperse heat generated by the resistor material. Nevertheless, surface mount components conventionally adhere to printed circuit boards (PCBs), posing challenges in achieving magnetic flux cancellation akin to coaxial shunt resistors. As shown in Fig. 1, the model illustrates a surface-mounted component adhered to a printed circuit board [5].

To enhance bandwidth, it is necessary to determine the values of multiple resistors and interconnect the sensing lines within the region of weakest magnetic flux density. However, in certain investigations, particularly those involving a resistance of 0.1 Ω , the documented analog measurement bandwidth remains below 200 MHz, accompanied by a transient current measurement error of 38% [6].

Further refinements to this methodology have been realized by partitioning the parallelors into two groups with a gap left in between, thereby engendering a region of weaker field [7]. This approach has yielded a simulated bandwidth exceeding 500 MHz, albeit at the expense of escalating the resistance to 1.0 Ω . Some researchers have explored the placement of surface mount resistors in radial or coaxial configurations, yet measurement bandwidth remains unreported [8]. Zhang et al. recently published a pioneering study unveiling the Surface-Mounted Distributed Coaxial Structure Resistor (SMDCSR), a novel resistor design [5]. This innovative approach achieves a compact coaxial structure while ensuring minimal transient temperature elevation. By encircling resistors within a circular configuration, the design emulates a coaxial structure, effectively mitigating the adverse effects of magnetic flux coupling. At the heart of the SMDCSR design lies the

Fig. 1 Surface mount coaxial shunt resistor PCB design [5]. Figure Copyright © 2021 IEEE Energy Convers. Congr. Expo. Publishing, Open Access

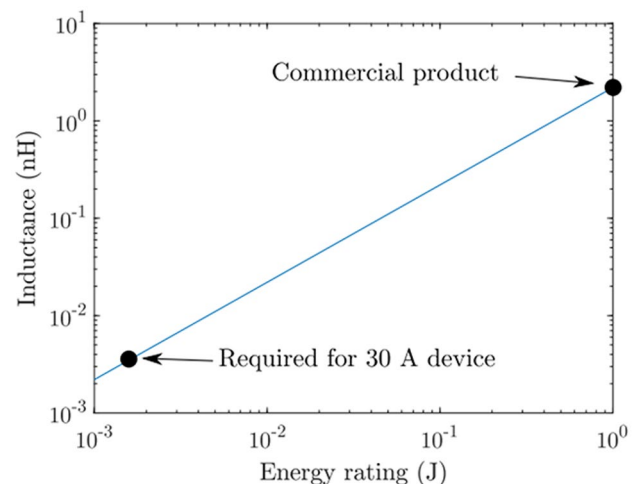


strategic reduction of inter-resistor gaps, enabling an impressive measurement bandwidth of up to 2.23 GHz. Leveraging diminutive 0402 resistors, the design significantly diminishes parasitic inductance, with optimal values plummeting as low as 0.12 nH. The relationship between the rated energy of coaxial shunt resistors and their parasitic inductance is shown in Fig. 2. Even when factoring in additional power loop area in worst-case scenarios, the cumulative inductance remains below 0.60 nH. This remarkable feat not only facilitates the achievement of high bandwidth and low inductance but also ensures measurement uncertainty is kept below 0.90%, even under more rigorous thermal distribution conditions compared to conventional methodologies. In essence, the SMDCSR design harnesses commercially available, cost-effective components to cater to the demands of wide-bandgap semiconductor dynamic characterization. This approach presents a versatile solution for realizing high bandwidth and low inductance in resistor current sensors. Furthermore, there is ample room for further refinement to streamline assembly processes and facilitate large-scale production.

Another type of current sensor indirectly measures the magnitude and direction of the current through the magnetic field it generates. It uses the amperometric loop law and has electrical insulation on both the primary and secondary sides. In the industrial field, five main types of current sensors are commonly used: (a) the Hall current sensor, (b) magnetic flux-gate current sensors, (c) magnetoresistive (MR) current sensors, which include AMR, GMR, and TMR, (d) Rogowski coils, and (e) current transformers.

Beyond direct measurement methods, various current sensing technologies have been extensively studied, leveraging the integration of magnetic fields and diverse physical principles. These methodologies exploit phenomena including the Faraday effect, magneto-optical effect, nuclear magnetic resonance (NMR), quantum Hall effect, among others [9–12]. Each avenue boasts unique attributes, catering to distinct market segments with differing cost structures, thereby complicating their utilization landscape. While certain technologies remain nascent or are confined to niche applications due to their high cost and demanding operational environments, others, such as those based on the Faraday magneto-optical effect, excel in measuring large AC currents up to 100 kA, albeit encountering challenges with DC measurements. In contrast, current sensors employing the loop amperometric law circumvent primary and secondary electrical insulation issues inherent in other designs. This mature technology, amenable to mass production and competitively priced, enjoys widespread adoption. This paper delves into the technical underpinnings, realization methodologies, as well as the merits and limitations of this class of current sensors, offering insights into their diverse applications.

Fig. 2 Relationship between coaxial shunt resistor energy rating and its parasitic inductance [5]. Figure Copyright © 2021 IEEE Energy Convers. Congr. Expo. Publishing, Open Access



This study focuses on loop-based current sensors. Demonstrating technical maturity, scalability for mass production, and cost-effectiveness, these sensors enjoy pervasive adoption across industrial domains. The paper endeavors to elucidate the technical foundations, implementation strategies, as well as the inherent advantages and limitations characterizing this breed of current sensor technology.

2 Current measurement technique based on Ampere's law of loops

According to the amperometric loop law, the integral of the magnetic field strength h along a closed path C (of length L) is equivalent to the algebraic summation of the individual currents enclosed by the same closed path C , which is demonstrated in Fig. 3.

In the pursuit of quantifying the magnitude and direction of magnetic field strength H , two prevalent methodologies are employed. The first entails a direct assessment of the magnetic induction strength B engendered by the current, achieved through induction units like Hall effect sensors, magnetic flux gates, and magnetoresistive technologies. Alternatively, the second approach involves an indirect appraisal, gauging the alteration in magnetic field strength h induced by the current via measurement of the resultant voltage, leveraging Faraday's law of electromagnetic induction.

3 Current sensor based on amperometric loop law

Current sensors find classification into two distinct categories contingent upon their methodological approach to current measurement. The first category involves direct measurement of magnetic induction strength B , encompassing three subtypes: Hall current sensors, fluxgate current sensors and Magnetoresistive Current Sensors. The following sections will detail the principles and applications of the three aforementioned sensors.

3.1 Hall current sensor

Hall current sensors have garnered widespread adoption owing to their efficacy. Operating on the principle of measuring the magnetic induction strength (B) resultant from current flow, they subsequently employ signal processing algorithms to ascertain both the magnitude and direction of the current. These sensors hinge upon Hall sensing units that exploit the Hall effect, elegantly encapsulated within integrated circuits for seamless integration and enhanced performance.

The Hall effect was discovered in 1879 by Edwin Hall. This phenomenon occurs when a magnetic field strength B is applied to a rectangular conductor sheet perpendicular to the current I , generating an electric potential difference (e) under the Lorentz force [13], as shown in Fig. 4.

The selection of materials for Hall devices is crucial for the generation of the Hall effect. Silicon and III–V compounds (e.g., InSb, GaAs, InAs), which possess high mobility and relatively low conductivity, are commonly used in Hall Effect Current Sensor (HECS) devices [4, 5]. As early as 2011, Chen et al. reported a novel method for measuring power currents using coreless Hall effect current transformers (HCTs) [14]. This method eliminates environmental interference, particularly mitigating the magnetic fields generated by the other two phases in three-phase power systems, and Fig. 5 presents a cross-sectional view of a three-phase source. Consequently, it enables high-precision current measurements without the use of iron cores. Due to the absence of iron cores, HCTs are compact and flexible, thus avoiding the saturation issues

Fig. 3 Schematic diagram of Ampere's circuital law

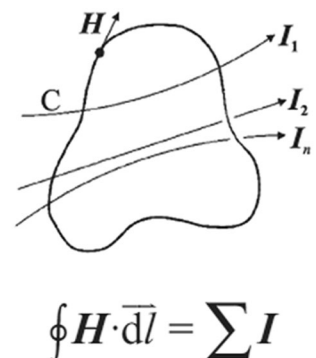
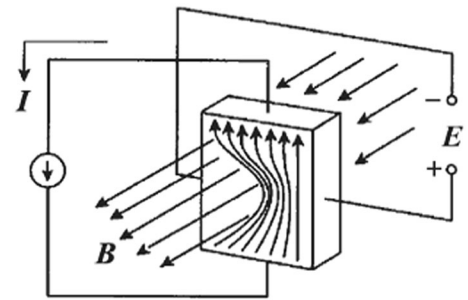


Fig. 4 Diagram of Hall effect working principle



commonly encountered with traditional current transformers (CTs). Therefore, replacing traditional CTs with HCTs can result in significant cost savings. Employing a magnetic core can effectively shunt stray magnetic fields around the sensor. In contrast, coreless architectures are vulnerable to stray fields from high-current traces, which may be captured by the Hall plates, leading to inaccurate current measurements. To mitigate this, a differential Hall plate configuration can be utilized; however, any mismatch between the Hall plates or any non-uniformity in the magnetic field can cause deviations in the output signal [15]. Over years of development, Hall sensors have achieved significant advancements. In 2024, it was reported that Hall sensors were applied in magnetic tactile sensors, greatly enhancing sensitivity and demonstrating exceptional performance with low hysteresis (6.82%), fast response time (< 2 ms), remarkable stability (0.09%), and high repeatability (0.48%). This research is poised to actively drive the development of tactile sensors, offering substantial applications in robotics, health monitoring, and electronic skin devices [16].

3.2 Magnetic flux gate current sensor

The magnetic flux gate stands as a supremely precise method for contemporary magnetic field measurements [17]. This approach hinges upon the employment of a magnetic flux gate sensing unit capable of discerning direct or low-frequency AC magnetic fields spanning the range of 10^{-10} to 10^{-4} T. The inception of this technique dates back to 1931 when Thomas was granted the first patent [18]. In the ensuing section, a comprehensive discourse on magnetic flux gating shall be furnished.

Fig. 5 Positions of the HCTs in different arrangements of cables. **a** Cross-sectional view of a three-phase source arranged vertically and parallel to each other in a plane, as shown in Fig. 1a. **b** Cross-sectional view of a three-phase source arranged in a regular triangle, as shown in Fig. 1b [14]. Figure Copyright © 2011 IEEE Energy Convers. Congr. Expo. Publishing, Open Access

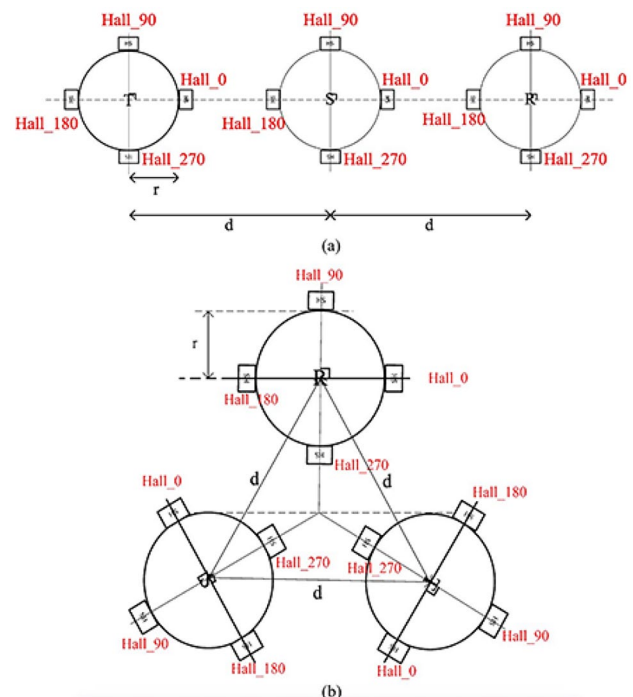


Fig. 6 Demonstration of fluxgate sensing unit

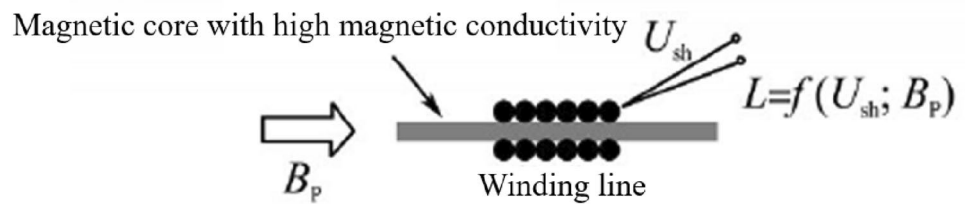
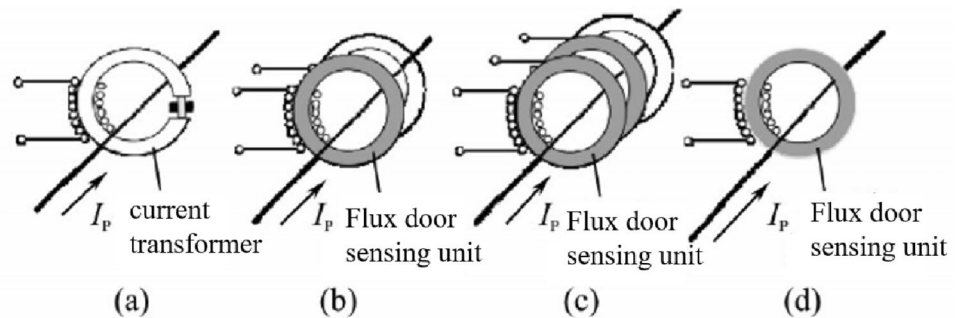


Fig. 7 Main types of fluxgate current transducer



3.2.1 Working principle of the standard magnetic flux gate current sensor

Standard magnetic flux gate current sensors rely on a magnetic flux gate sensing unit in conjunction with tailored signal processing for their operation. The configuration of this magnetic flux gate sensing unit is illustrated in Fig. 6. In the construction of the flux gate sensing unit, a slender strip of high-permeability material (μ) is meticulously wound around the magnetic core (R) using copper wire, thereby establishing an equivalent “saturated inductor” characteristic. The magnitude of inductance (L) within the magnetic flux gate sensing unit is contingent upon the magnetic conductivity of the magnetic core (μ_r), a parameter governed by factors such as coil turns and structural dimensions. Notably, when the magnetic induction strength (B) attains significant levels and saturates the magnetic core, the permeability (μ_r) diminishes, consequently yielding reduced inductance (L). Conversely, in scenarios where the magnetic induction strength (B) is diminished, a proportional increase in inductance (L) ensues.

3.2.2 Prevailing types of magnetic flux gate current sensors

There are four types of mainstream magnetic flux gate current sensors [19], as shown in Fig. 7.

Figure 7b portrays a magnetic flux gate current sensor featuring two magnetic cores, renowned for its heightened performance relative to conventional magnetic flux gates. This augmented efficacy stems from two key factors: firstly, the segregation of the magnetic flux gate sensing unit onto a distinct magnetic core, thereby obviating any apertures that might compromise precision; secondly, the positioning of current transients, which bolster high-frequency performance, onto a separate magnetic core devoid of apertures. Figure 7c depicts a flux gate current sensor featuring three magnetic cores, distinguished by its superior performance compared to the two-core design, attributable to several factors: (i) the inclusion of two flux gate sensing units and two ring excitation coils oriented in opposing directions; (ii) refinement of the design of the high-frequency current transducer and processing circuit; and (iii) mitigation of interference stemming from induced voltage on the original edge current.

Figure 7d delineates the low-frequency magnetic flux gate current sensor. In low-frequency measurements, solely the low-frequency segment of the magnetic flux gate showcased in Fig. 11b was utilized, devoid of current transients and processing circuits. This strategic approach guarantees the attainment of precise and dependable output.

3.2.3 Performance

Comparing the performance of magnetic flux gate current sensors proves challenging owing to their diverse structures and product designs. Generally, these sensors boast attributes including low zero drift, high precision, remarkable resolution and sensitivity, expansive measurement and temperature ranges, as well as ample bandwidth and rapid response

Fig. 8 The detection circuit of Fluxgate current sensor [20]. Figure Copyright © 2022 IEEE Energy Convers. Congr. Expo. Publishing, Open Access

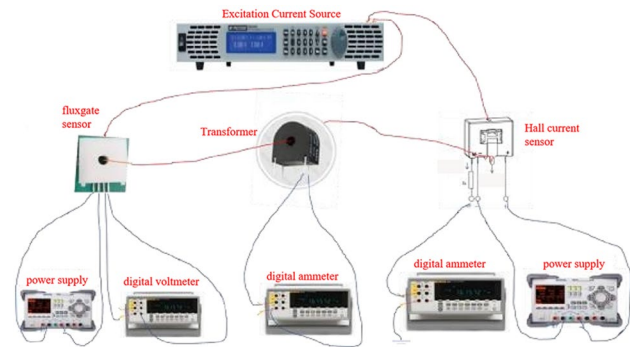
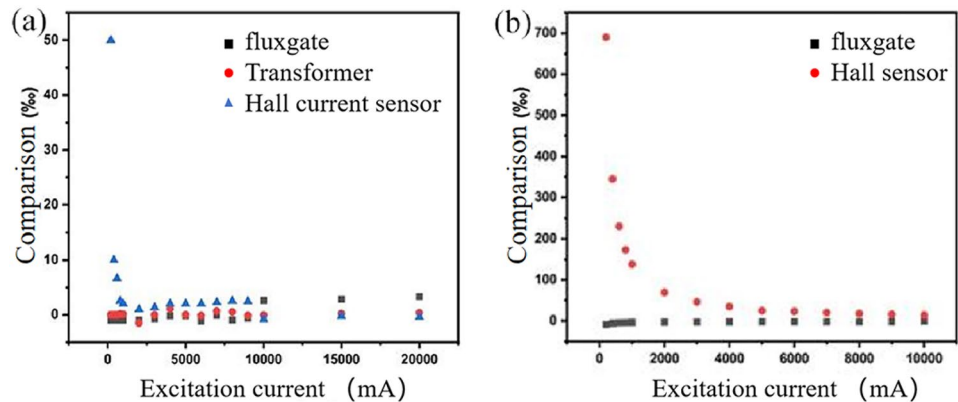


Fig. 9 a The test results of the traditional current transformer for alternating current; **b** the test results of the hall current sensor for alternating current [20]. Figure Copyright © 2022 IEEE Energy Convers. Congr. Expo. Publishing, Open Access



times. Despite these merits, magnetic flux gate current sensors encounter limitations, such as constrained bandwidth in low-frequency options, the potential for retro-feedback of voltage noise into the original circuit, noisy output at the excitation voltage frequency, and elevated current consumption. Given the high sensitivity of the magnetic flux gate sensing unit, measurements with these sensors span a broad spectrum, ranging from a few milliamperes to several kiloamperes.

In 2022, Wang et al. reported a study on the characteristics of magnetic flux gate current sensors [20]. Figure 8 illustrates the detection circuit of the magnetic flux gate current sensor. To construct the testing circuit as depicted in Fig. 8, a stabilized power supply is utilized to power the sensor, a high-precision current source provides the test current, and a high-precision digital voltmeter measures the current. Simultaneously, comparative tests were conducted on traditional current transformers and Hall current sensors, as shown in Fig. 9. It is evident from these tests that the measurement accuracy of the magnetic flux gate current sensor is comparable to that of current transformers and far superior to Hall current sensors. Furthermore, it is capable of measuring direct current, overcoming the limitation of current transformers in measuring direct current.

3.3 Magnetoresistive current sensor

In 1857, William Thomson unearthed the phenomenon of magnetoresistance in ferromagnetic materials [21]. These materials, comprising alloys of ferromagnetic elements, undergo alterations in resistance in reaction to fluctuations in the magnitude and orientation of the applied magnetic field. Despite this early discovery, commercialization was impeded by technical constraints until more than a century later, with the advent of thin film technology. Magnetoresistive sensing units, spanning various implementations and structural forms such as anisotropic magnetoresistance (AMR), giant magnetoresistance (GMR), and tunneling magnetoresistance (TMR), among others, exhibit a diverse landscape. To enhance precision in measurement and alleviate the effects of temperature drift, these units have been organized into a Wheatstone bridge configuration within. Furthermore, encapsulation within integrated circuits confers compactness upon these sensors. Originally employed to read magnetic recording media like tapes and hard disks, their utility has evolved to encompass the domain of amperometry.

Various magnetoresistive sensing units display unique characteristics, as outlined in Table 1. However, despite the substantially higher resistance change rates observed in GMR/TMR sensors compared to AMR sensors, they are constrained

by issues such as $1/f$ noise, non-linearity, and hysteresis [22]. Hence, there exists a pressing necessity to enhance their sensitivity and linear attributes.

3.3.1 Working principle of the MR sensing unit

Magnetoresistive sensing units are employed in various industries, and they differ in operating principles and implementation techniques. They include AMR, GMR, and TMR sensing units.

The AMR sensing unit operates based on the principles of magnetoresistance, wherein the resistance (R) of a ferromagnetic material, such as slope alloy, varies with the angle (θ) between the current direction (I) and the intrinsic magnetic field direction (M_0). The AMR sensor exhibits its lowest resistance when the current is perpendicular to M_0 and its highest resistance when the current is parallel to M_0 . By detecting the rate of change in resistance ($\Delta R/R$), the current can be indirectly determined. To enhance the sensitivity of the AMR resistance to magnetic field direction, a Barber Pole structure was implemented, ensuring $\theta = 45^\circ$, as illustrated in Fig. 10.

Figure 11 illustrates the relationship between the angle θ formed by the magnetic field M_0 , current I , the ratio R/R , and the rate of change in resistance $\Delta R/R$. The rate of resistance change $\Delta R/R$ varies among different magnetic materials, typically falling within the range of 2% to 4% [17, 23].

As depicted in Fig. 12, resistance variation in anisotropic magnetoresistance (AMR) hinges on the angle (θ) between the electric current and the metal's magnetization intensity. AMR originates from the interaction effects between magnetization and electron spin-orbit coupling. In ferromagnetic metals exhibiting positive AMR, such as nickel (Ni), the resistance reaches its maximum when the magnetization direction is parallel to the current, and its minimum when the magnetization is perpendicular to the current [22, 24]. Since the 1970s, AMR has been widely utilized in the recording industry.

The resistivity of the material is at its minimum when the magnetic moments of the ferromagnetic layers are aligned parallelly. Conversely, it is at its highest when the magnetic moment of the ferromagnetic layer is anti-parallel. The orientation of the magnetic moment is regulated by the alteration of the external magnetic field. In order to minimize temperature drift, we incorporated the GMR sensing unit into a Wheatstone bridge structure, which typically has two variations: (a) a magnetically shielded GMR sensing unit, and (b) a spin valve GMR sensing unit. Figure 13 illustrates the magnetically shielded variation [25].

The GMR resistance of all four arms of the Wheatstone bridge underwent identical processing steps, ensuring uniformity. This included applying a consistent temperature coefficient to mitigate temperature-induced drift. Shielding with permalloy was employed for resistors R_2 and R_3 to insulate them from external magnetic influences, rendering them suitable as reference resistors. In contrast, the resistance values of measured resistors R_1 and R_4 fluctuated with changes in the external magnetic field. The shielding material, characterized by widths D_2 and void width D_1 , served to amplify the magnetic field generated by the current under test by a magnification factor approximately equal to D_2/D_1 . Adjusting the widths of D_1 and/or D_2 allowed for tuning the sensitivity of the GMR. Although the GMR sensing unit consistently produced a positive output, practical applications necessitated an externally biased magnetic field to detect both the magnitude and direction of the current, as illustrated in Fig. 14.

The giant magnetoresistance (GMR) phenomenon was discovered in the 1980s. It was observed in multilayer systems composed of Fe and Cr. The revelation of GMR sparked numerous experimental and theoretical investigations due to its ability to induce significant changes in resistance (ΔR) under relatively small magnetic fields, albeit often requiring extremely low temperatures [26, 27]. As depicted in Fig. 15, the typical structure of magnetic multilayer systems consists of ferromagnetic layers separated by non-magnetic (or non-ferromagnetic) layers. GMR is attributed to spin-dependent scattering, initiated by the spin polarization of electrons in the presence of an external magnetic field [28–30]. When the magnetization directions of the two ferromagnetic layers are antiparallel, a high resistance state is observed, whereas a low resistance state is observed when they are parallel. The advent of GMR had a transformative impact on magnetic storage devices, notably enhancing the storage capacity of technologies such as Hard Disk Drives (HDDs). This newfound understanding and control over magnetoresistive properties paved the way innovations in data storage and magnetic sensing technologies, contributing significantly to the evolution of modern computing and information storage systems.

The Tunneling Magnetoresistance (TMR) effect is a phenomenon rooted in the spin-dependent transport of electrons, presenting a paradigm similar to that of Giant Magnetoresistance (GMR). However, TMR diverges by replacing the non-magnetic conductive layer in GMR with an exceedingly thin insulating layer, crafting an FM/IFM junction. This junction features two layers of ferromagnetic material brought proximate by traversing the insulating layer through the quantum tunneling effect. The magnitude of the ensuing tunneling current hinges upon the relative orientation of

Table 1 Performance comparison of AMR, GMR, TMR sensing unit

| Sensor chip | Structure | Magneto-resistive ratio ($\Delta R/R_{\min}$)/% | Typical signal amplitude/ (mV V ⁻¹) | Output temperature coefficient/ (% °C ⁻¹) | Zero offset output/ (mV V ⁻¹) | Zero temperature drift coefficient/ ($\mu\text{V V}^{-1} \text{ } ^\circ\text{C}^{-1}$) | Magnetic field dynamic range/ (kA m ⁻¹) | Operating temperature range/°C | Signal-to-noise ratio/ dB | Integrability |
|-------------|-----------|---|--|--|--|--|--|--------------------------------|------------------------------|------------------|
| AMR | Bridge | 3 | 1.5 | -0.35 | ±2 | ±2 | 1–10 | -40 to +150 | 65 | Easy integration |
| GMR | Bridge | 15 | 1.5 | -0.1 | ±64 | ±5 | 2–50 | -40 to +150 | 70 | Easy integration |
| TMR | Bridge | 50–300 | 15 | -0.1 | ±3 | ±3 | 1–100 | -40 to +200 | 90 | Easy integration |

Fig. 10 Barber pole structure of basic AMR sensing unit

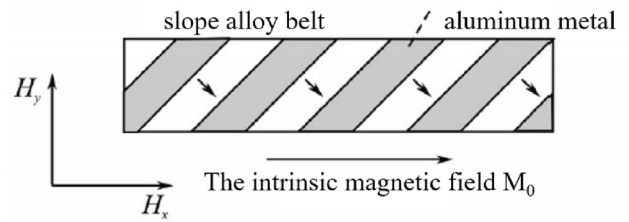


Fig. 11 $\Delta R/R$ related to the angle θ between the magnetization M_0 and the current I

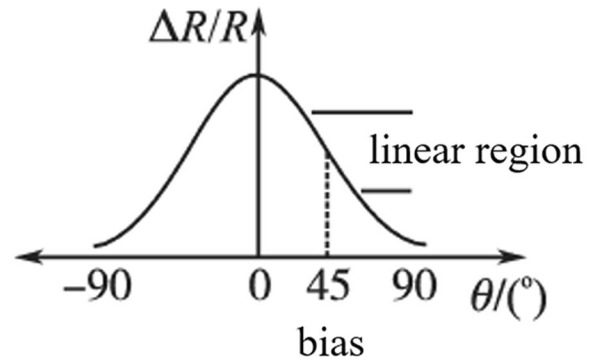


Fig. 12 AMR schematic diagram [22]. Figure Copyright © 2021 Chemosensors Publishing, Open Access

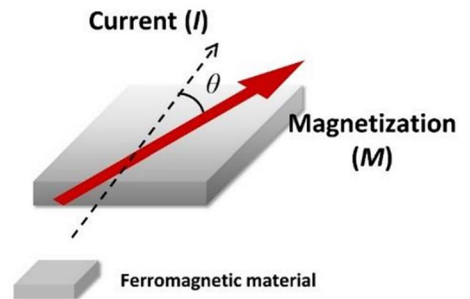


Fig. 13 Diagram of GMR wheatstone bridge and its equivalent circuits

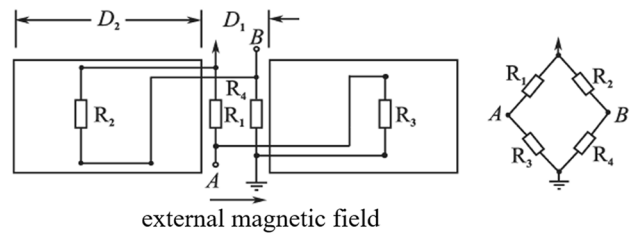


Fig. 14 GMR sensing unit output versus applied bias magnetic field

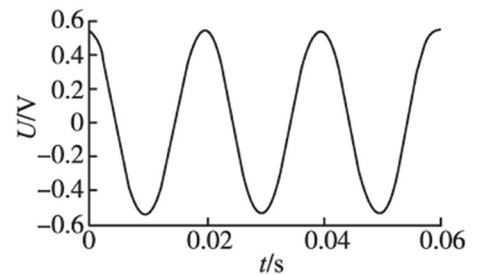
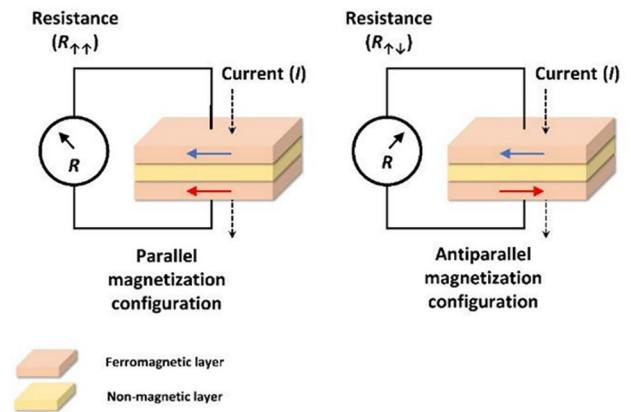


Fig. 15 GMR schematic diagram [22]. Figure Copyright © 2021 Chemosensors Publishing, Open Access



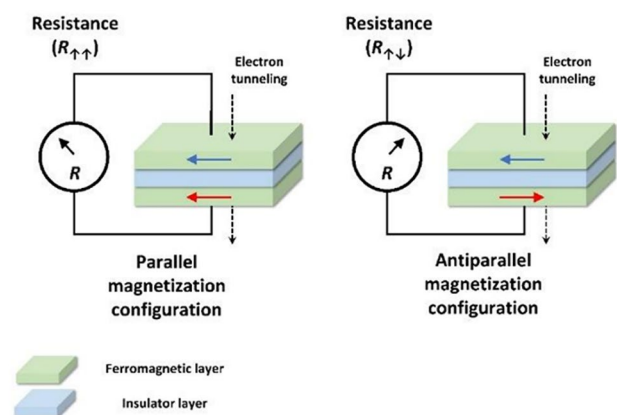
their magnetizations [29]. Consequently, a TMR sensing unit experiences a magnetic resistance metamorphosis in reaction to fluctuations in the external magnetic field, and the ascertained current is deduced indirectly from this magnetic resistance variation.

Following the discovery of giant magnetoresistance (GMR), tunneling magnetoresistance (TMR) quickly emerged as a significant research focus. In practical applications, TMR, akin to GMR, features a magnetic multilayer structure. The fundamental unit of the TMR multilayer system is the magnetic tunnel junction (MTJ), as illustrated in Fig. 16 [31]. Quantum tunneling allows electrons to traverse from one side of the insulator to the other. The magnetization direction of the ferromagnetic layers in TMR is pivotal; spin-dependent tunneling effects enable electrons to tunnel into subbands with matching spin orientations. Consequently, resistance varies with changes in spin subbands induced by magnetization intensity [32]. During its early development, TMR demonstrated substantial resistance changes (ΔR , 30%) even at low temperatures.

3.3.2 Magnetoresistive (MR) current sensors

Magnetoresistive current sensors employ a magnetoresistive sensing unit (AMR, GMR, or TMR) to gauge both the amplitude and direction of the current. Within this realm, two distinct categories emerge: open-loop and closed-loop sensors, each distinguished by unique operational principles and performance attributes. Open-loop magnetoresistive (MR) current sensors are adept at measuring not only direct currents but also alternating and intricate current waveforms. Open-loop current sensors, while versatile in measuring various currents, encounter several challenges. These include the necessity for online tuning to achieve high precision, a reduction in measurement accuracy due to the skin effect of the current, susceptibility to external magnetic field interference, and the need for magnetic shielding using materials with high magnetic permeability and electrical conductivity, which complicates the structure and increases costs. In contrast, closed-loop MR current sensors offer distinct advantages over their open-loop counterparts. They exhibit minimal or no magnetic offset, ensuring high accuracy and excellent linearity. Additionally, they boast fast response times and broad bandwidths. Nonetheless, they also possess limitations, including higher power consumption, susceptibility to external

Fig. 16 Tunnel magnetoresistance (TMR) schematic diagram [22]. Figure Copyright © 2021 Chemosensors Publishing, Open Access



magnetic field interference (especially in the case of Anisotropic Magnetoresistance, or AMR sensors), larger size and higher costs (particularly for Giant Magnetoresistance, GMR, and Tunneling Magnetoresistance, TMR, sensors). In terms of measuring large currents, the measurement range of loop MR current sensors parallels that Hall effect closed-loop current sensors. They are capable of detecting currents ranging from milliamps to 20 kiloamps, offering a comprehensive solution across broad spectrum of current magn.

Since the discovery of magnetoresistive (MR) effects, various MR materials and structures have been developed to achieve optimal performance under different conditions. Due to their unique anisotropic properties, AMR materials have been utilized in designing memory sensors and angle sensors [33–35]. However, the MR of AMR materials is relatively low (2.5–5%) [36]. In recent years, emerging nanotechnologies have provided a variety of options for constructing ideal magnetic resonance materials and structures. Currently, magnetic resonance sensors find primary applications in magnetic storage, position sensing, current sensing, non-destructive testing, and biomedical sensing systems. Additionally, MR sensors are utilized in anti-lock braking systems, cardiac mapping, and electrical isolators [37, 38]. Due to its unique physical and chemical properties, graphene has quickly garnered attention from researchers [39]. Multilayer graphene, graphene foam, and hybrid graphene nanposites have been introduced into the development of magnetic resonance materials and structures [40–42]. At ambient temperature or extremely low temperatures (1.9 K), magnetic resonance systems based on single-layer graphene, bilayer graphene, and multilayer graphene (Fig. 17) have been observed to exhibit significant magnetoresistance [43, 44].

In most scenarios, the fabrication of layered graphene systems necessitates specific substrates, manufacturing methodologies, and meticulous layer control, thereby amplifying the intricacies and expenses associated with the production process. The attainment of desirable magnetic rheological characteristics at ambient temperatures poses a significant hurdle. Despite the emergence of certain methodologies aimed at enhancing the performance of layered graphene systems at room temperature, their reliance on bespoke instrumentation prolongs processes and undermines cost-effectiveness. Moreover, augmenting the magnetic resonance phenomenon under low-magnetic-field ambient conditions and streamlining the preparation protocols for magnetic resonance materials prove to be formidable challenges. Nonetheless, a breakthrough in these technologies is poised to enhance the efficacy of integrated magnetic resonance unit devices while concurrently curtailing production expenditures. Such advancements would mitigate prevailing obstacles encountered by magnetic resonance sensors and propel the trajectory of their future applications. In sum, while graphene exhibits prodigious promise within the realm of magnetic resonance, further strides in technology and innovation are imperative to actualize its widespread adoption.

In addition to graphene's widespread application in Tunneling Magnetoresistive Current Sensors, in 2024, Qi et al. reported a novel tunneling magnetoresistance-based current sensor relying on a reference magnetic field source [45]. The experimental principle, illustrated in Fig. 18, delves into the linearity, hysteresis, error, and stability of the sensor. The findings reveal that within the 1 to 10 A range, the chip's error is less than 1.46%, markedly lower than that of TMR chips. Moreover, given that the reference alternating magnetic flux density is considerably smaller than the magnetic flux density produced by the primary current, its power consumption can be disregarded. The principle entails generating a minor reference alternating magnetic flux via a coil, akin to a disturbance induced by the magnetic flux from the primary current. TMR chips can also detect this reference alternating magnetic flux, serving to compensate for the magnetic hysteresis error of the TMR chips. This innovative current sensor boasts simplicity, affordability, low power consumption, and high accuracy, potentially propelling the industrial advancement of current sensors.

Fig. 17 **a** Schematic diagram of the fabrication process of multilayer graphene/metal catalyst heterojunction. **b** MR of the response of multilayer graphene on Cu substrate [44]. Figure Copyright © 2013 MDPI Publishing, Open Access

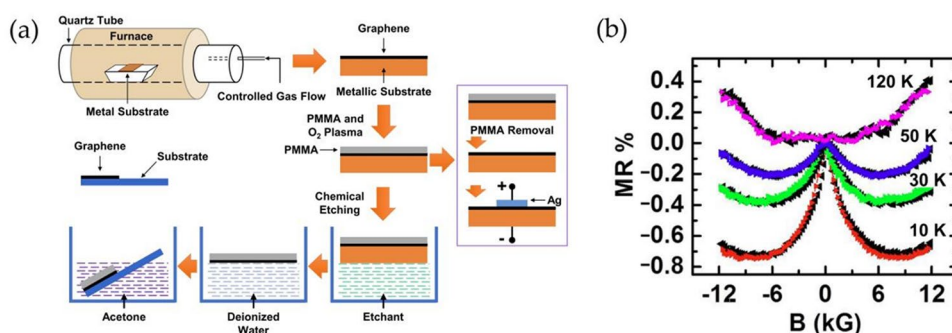
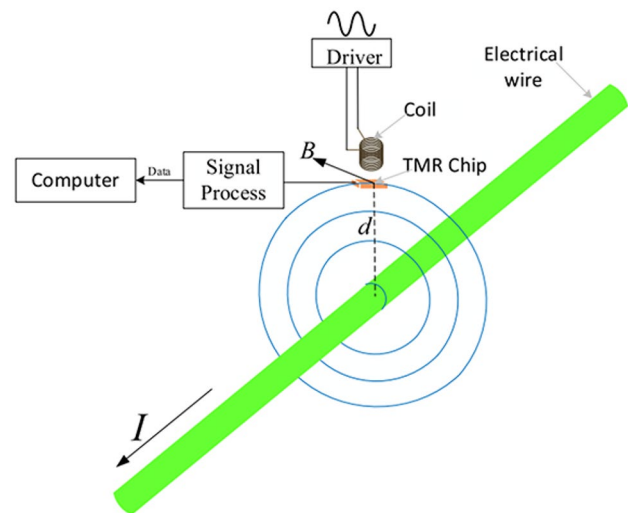


Fig. 18 Principle of the proposed TMR sensor [45]. Figure Copyright © 2024 IEEE Energy Convers. Congr. Expo. Publishing, Open Access



4 Conclusion

Shunts grounded in Ohm's law and current sensors rooted in diverse physical principles provide a spectrum of functionalities, encompassing varied measurement ranges, precision, bandwidth, insulation, response speed, interference resistance, and cost-effectiveness. Over time, strides in measurement technology perpetually propel advancements across diverse industrial sectors.

The voltage output across the terminals of a shunt is directly proportional to the current being measured, rendering these sensors advantageous due to their affordability and simplicity, aligning well with the basic needs of current measurement applications. Nonetheless, when shunts are connected in series within a circuit, they introduce notable limitations. Overcoming these constraints necessitates additional measures, often resulting in increased expenses and decreased bandwidth. The development of SMDCSR (Serially-Connected Multi-Directional Current Sensing Resistor) addresses these challenges by minimizing the gaps between resistors, thereby augmenting bandwidth while concurrently reducing inductance. Moreover, there exists significant potential for enhancements aimed at streamlining assembly processes and facilitating mass production.

Current sensors based on the loop ampere law circumvent inherent primary and secondary electrical insulation issues present in other designs. This mature technology is well-suited for mass production, boasting competitive pricing and widespread adoption. In the realm of Hall current sensors, the Coreless Hall Effect Current Transformer (HCT) enables high-precision current measurements. With its absence of a core, the HCT is compact and flexible, mitigating the saturation problems commonly encountered with traditional Current Transformers (CTs). However, coreless architectures are susceptible to stray fields from high-current conductors, leading to inaccurate current measurements. In recent research findings, the application of Hall sensors in magnetic tactile sensors has significantly enhanced sensitivity, showcasing outstanding attributes such as low hysteresis, rapid response times, high stability, and repeatability. This research holds promise for driving the advancement of tactile sensors, offering substantive applications in robotics, health monitoring, and electronic skin devices. The integration of Hall current sensors is poised to propel industrial development in the future.

Magnetic flux gates represent an exceptionally precise method for contemporary magnetic field measurements. Generally, such sensors exhibit attributes including low zero drift, high accuracy, outstanding resolution and sensitivity, wide measurement and temperature ranges, as well as ample bandwidth and rapid response times. Despite these advantages, magnetic flux gate current sensors encounter limitations such as restricted bandwidth in low-frequency options, the potential for voltage noise to feed back inversely into the primary circuit, noise output at excitation voltage frequencies, and increased current consumption. The measurement accuracy of magnetic flux gate current sensors rivals that of current transformers and far surpasses that of Hall current sensors. Additionally, they are capable of measuring direct current, overcoming the limitations of current transformers in measuring DC.

Since the discovery of the magnetoresistance (MR) effect, researchers have been exploring various MR materials and structures to achieve optimal performance under different conditions. Graphene, with its unique physical and chemical

properties, quickly garnered attention from researchers. However, in most cases, manufacturing layered graphene systems requires specific substrates, fabrication methods, and precise layer control, thereby amplifying the complexity and costs associated with the production process. While some methods aimed at enhancing the performance of layered graphene systems at room temperature have emerged, their reliance on customized instruments prolongs the process and reduces cost-effectiveness. On the other hand, due to its unique anisotropic properties, Anisotropic Magnetoresistance (AMR) materials have been utilized in designing memory and angle sensors. However, the MR of AMR materials is relatively low (2.5–5%). Therefore, magnetic resistance current sensors based on AMR materials still face numerous challenges before commercialization. Nonetheless, there have been recent reports of a novel type of tunnel magnetoresistance current sensor based on a reference magnetic field source. This new type of current sensor features simplicity, low cost, low power consumption, and high accuracy, offering the potential to accelerate the industrial development of current sensors.

Author contributions Chunjun Tang: writing, analyze data. Jiakai Liang, Qiang Zhu: analyze data. Xiaofeng Lu: propose a concept. Jun Shu: data collection. Cong Jiang: revise the paper.

Data availability The data that support the findings of this study are available from the corresponding author upon reasonable request.

Declarations

Competing interests The authors declare that they have no known competing financial interests or personal relationships that could have appeared to influence the work reported in this paper.

Open Access This article is licensed under a Creative Commons Attribution 4.0 International License, which permits use, sharing, adaptation, distribution and reproduction in any medium or format, as long as you give appropriate credit to the original author(s) and the source, provide a link to the Creative Commons licence, and indicate if changes were made. The images or other third party material in this article are included in the article's Creative Commons licence, unless indicated otherwise in a credit line to the material. If material is not included in the article's Creative Commons licence and your intended use is not permitted by statutory regulation or exceeds the permitted use, you will need to obtain permission directly from the copyright holder. To view a copy of this licence, visit <http://creativecommons.org/licenses/by/4.0/>.

References

1. Bedareva EV, Marinushkin PS, Khudonogova LI. Calculation of coaxial shunts superheat temperature. *IOP Conf Ser Mater Sci Eng.* 2014;66:1–5.
2. Current Viewing Resistors. T&M research, Albuquerque, NM, USA. 2020. <http://www.tandmresearch.com/>.
3. Zhang W, Zhang Z, Wang F. Review and bandwidth measurement of coaxial shunt resistors for wide-bandgap devices dynamic characterization. In: *Proc. IEEE Energy Convers. Congr. Expo.* 2019. p. 3259–64.
4. Precision thin film technology. Vishay, Malvern, PA, USA. 2020. www.vishay.com.
5. Zhang W, Zhang Z, Wang F, Brush EV, Forcier N. High-bandwidth low-inductance current shunt for wide-bandgap devices dynamic characterization. *IEEE Energy Convers Congr Expo.* 2021;36:4522–31.
6. Danilovic M, Chen Z, Wang R, Luo F, Boroyevich D, Mattavelli P. Evaluation of the switching characteristics of a gallium-nitride transistor. In: *Proc. IEEE Energy Convers. Congr. Expo.* 2011. p. 2681–8.
7. Hernandez JC, Petersen LP, Andersen MAE, Petersen NH. Ultrafast switching superjunction MOSFETs for single phase PFC applications. In: *Proc. 29th Annu. Appl. Power Electron. Conf. Expo.* 2014. p. 143–9.
8. Joannou AJL, Pentz DC, van Wyk JD, de Beer AS. Some considerations for miniaturized measurement shunts in high frequency power electronic converters. In: *Proc. 16th Eur. Conf. Power Electron. Appl.* 2014. p. 1–7.
9. Schatz PN, McCaffery AJ. The Faraday effect. *Q Rev Chem Soc.* 1969;23:552–84.
10. Pershan PS. Magneto-optical effects. *J Appl Phys.* 1976;38:1482–90.
11. Hatzakis E. Nuclear magnetic resonance (NMR) spectroscopy in food science: a comprehensive review. *Compr Rev.* 2019;18:189–220.
12. von Klitzing K. Developments in the quantum Hall effect. *R Soci.* 2005;363:1471–2962.
13. Mammano B. Current sensing solutions for power supply designer. In: *Power Design Seminar SEM 1200*, Unirode Corp. 1997. p. 8–10, 15.
14. Chen K, Chen N. A new method for power current measurement using a coreless Hall effect current transformer. *IEEE Energy Convers Congr Expo.* 2011;60:158–69.
15. Crescentini M, Syeda SF. Hall-effect current sensors: principles of operation and implementation techniques. *IEEE Energy Convers Congr Expo.* 2022;22:10137–51.
16. Li XJ, Deng R, Jiao WL, Xu SZ, Xie HK, Han D, Wang XY. A high-sensitivity magnetic tactile sensor with a structure-optimized Hall sensor and a flexible magnetic film. *IEEE Energy Convers Congr Expo.* 2024;24:15935–44.
17. Lenz J, Edelstein AS. Magnetic sensors and their applications. *IEEE Sens J.* 2006;6(3):631–49.
18. Ripka P. Review of fluxgate sensors. *Sens Actuators A Phys.* 1992;33(3):129–41.

19. Isolated current and voltage transducers: characteristics-applications-calculations. 3rd edition. http://www.lem.com/images/stories/files/Products/P1_5_1_industry/CH24101E.pdf. Accessed 15 Aug 2017.
20. Wang SP, Lu CG, Song L, Chen YN, Fu Z, Liu F, Huang HH. Research on characteristics of a high precision current sensor. In: IEEE Energy Convers. Congr. Expo. 2022. p. 10–13.
21. Tumanski S. Thin film magnetoresistive sensors. Boca Raton: CRC Press; 2001.
22. Yang SL, Zhang J. Current progress of magnetoresistance sensors. *Chemosensors*. 2021;9:211.
23. Laimer G, Kolar JW. Design and experimental analysis of a DC to 1 MHz closed loop magnetoresistive current sensor. In: Proc. Appl. Power Electron. Conf. Exposition, APEC2005, Austin, TX, 2005, vol. 2. p. 1288–92.
24. Campbell IA, Fert A. Chapter 9 Transport properties of ferromagnets. In: Handbook of ferromagnetic materials, vol. 3. Elsevier: Amsterdam; 1982. p. 747–804.
25. Caruso MJ, Smith CH, Bratland T, et al. A new perspective on magnetic field sensing. *Sensors*. 1998;1(15):34–47.
26. Baibich MN, Broto JM, Fert A, Van Dau FN, Petroff F, Etienne P, Creuzet G, Friederich A, Chazelas J. Giant magnetoresistance of (001)Fe/(001)Cr magnetic superlattices. *Phys Rev Lett*. 1988;61:2472–5.
27. Binasch G, Grünberg P, Saurenbach F, Zinn W. Enhanced magnetoresistance in layered magnetic structures with antiferromagnetic inter-layer exchange. *Phys Rev B*. 1989;39:4828–30.
28. Chappert C, Fert A, Van Dau FN. The emergence of spin electronics in data storage. *Nat Mater*. 2007;6:813.
29. Zahn P, Binder J, Mertig I, Zeller R, Dederichs PH. Origin of giant magnetoresistance: bulk or interface scattering. *Phys Rev Lett*. 1998;80:4309–12.
30. Fert A, Campbell IA. Two-current conduction in nickel. *Phys Rev Lett*. 1968;21:1190–2.
31. Inoue J, Maekawa S. Theory of tunneling magnetoresistance in granular magnetic films. *Phys Rev B*. 1996;53:R11927–9.
32. Zhu J-G, Park C. Magnetic tunnel junctions. *Mater Today*. 2006;9:36–45.
33. Demirci E. Magnetic and magnetotransport properties of memory sensors based on anisotropic magnetoresistance. *J Supercond Novel Magn*. 2020;33:3835–40.
34. Sreevidya PV, Borole UP, Kadam R, Khan J, Barshilia HC, Chowdhury P. A novel AMR based angle sensor with reduced harmonic errors for automotive applications. *Sens Actuators A*. 2021;324: 112573.
35. Guo Y, Deng Y, Wang SX. Multilayer anisotropic magnetoresistive angle sensor. *Sens Actuators A Phys*. 2017;263:159–65.
36. Fullerton EE, Childress JR. Spintronics, magnetoresistive heads, and the emergence of the digital world. *Proc IEEE*. 2016;104:1787–95.
37. Giebler C, Adelerhof DJ, Kuiper AET, van Zon JBA, Oelgeschläger D, Schulz G. Robust GMR sensors for angle detection and rotation speed sensing. *Sens Actuators A*. 2001;91:16–20.
38. Rieger G, Ludwig K, Hauch J, Clemens W. GMR sensors for contactless position detection. *Sens Actuators A*. 2001;91:7–11.
39. Novoselov KS, Colombo L, Gellert PR, Schwab MG, Kim K. A roadmap for graphene. *Nature*. 2012;490:192–200.
40. Chen J-J, Meng J, Zhou Y-B, Wu H-C, Bie Y-Q, Liao Z-M, Yu D-P. Layer-by-layer assembly of vertically conducting graphene devices. *Nat Commun*. 1921;2013:4.
41. Sagar RUR, Qazi HIA, Zeb MH, Stadler FJ, Shabbir B, Wang X, Zhang M. Tunable sign of magnetoresistance in graphene foam—Ecoflex® composite for wearable magnetoelectronic devices. *Mater Lett*. 2019;253:166–70.
42. Zhu J, Luo Z, Wu S, Haldolaarachchige N, Young DP, Wei S, Guo Z. Magnetic graphene nanocomposites: electron conduction, giant magnetoresistance and tunable negative permittivity. *J Mater Chem*. 2012;22:835–44.
43. Wu H-C, Chaika AN, Hsu M-C, Huang T-W, Abid M, Abid M, Aristov VY, Molodtsova OV, Babenkov SV, Niu Y, et al. Large positive in-plane magnetoresistance induced by localized states at nanodomain boundaries in graphene. *Nat Commun*. 2017;8:14453.
44. Bodepudi SC, Singh AP, Pramanik S. Current-perpendicular-to-plane magnetoresistance in chemical vapor deposition-grown multilayer graphene. *Electronics*. 2013;2:315–31.
45. Qi ZX, Wei P, Liu CQ, Huang H, Xu HF, Li XL. A novel tunneling magnetoresistive current sensor based on reference magnetic field source. *IEEE Energy Convers Congr Expo*. 2024;8:5500304.

Publisher's Note Springer Nature remains neutral with regard to jurisdictional claims in published maps and institutional affiliations.